Kinetics of Actin Elongation and Depolymerization at the Pointed End†

Annemarie Weber,*,‡ Jennifer Northrop,‡ Marilyn F. Bishop,§,∥ Frank A. Ferrone,§ and Mark S. Mooseker⊥

Pennsylvania Muscle Institute, University of Pennsylvania, Philadelphia, Pennsylvania 19104, Department of Physics and Atmospheric Science, Drexel University, Philadelphia, Pennsylvania 19104, and Department of Biology, Yale University, New Haven, Connecticut 06511

Received January 13, 1986; Revised Manuscript Received December 2, 1986

ABSTRACT: We measured the rate of elongation at the pointed filament end with increasing concentrations of G-actin [$J(c)$ function] using villin-capped actin filaments of very small (actin/villin = 3, VA_3) and relatively large size (actin/villin = 18, VA_{18}) as nuclei for elongation. The measurements were made under physiological conditions in the presence of both Mg^{2+} and K^+. In both cases the $J(c)$ function was nonlinear. In contrast to the barbed filament end, however, the slope of the $J(c)$ function sharply decreased rather than increased when the monomer concentration was lowered to concentrations near and below the critical concentration c_∞. At zero monomer concentration, depolymerization at the pointed end was very slow with a rate constant of 0.02 s^{-1} for VA_{18}. When VA_3 was used, the nonlinearity of the $J(c)$ function was greatly exaggerated, and the nuclei elongated at actin concentrations below the independently measured critical concentration for the pointed end. This is consistent with and confirms our previous finding [Weber, A., Northrop, J., Bishop, M. F., Ferrone, F. A., & Mooseker, M. S. (1987) *Biochemistry* (preceding paper in the issue)] that at an actin–villin ratio of 3 a significant fraction of the villin is free and that a series of steady states exist between villin–actin complexes of increasing size and G-actin. The rate constant of elongation seems to increase with increasing G-actin concentrations because of increasing conversion of free villin into villin–actin oligomers during the period of the measurement of the initial elongation rate. The villin–actin oligomers have a much higher rate constant of actin binding than does free villin. By contrast, villin–actin oligomers of an average size of 18 actin molecules per villin (VA_{18}) do not coexist with significant free villin (and consequently do not elongate at G-actin concentrations below the independently measured c_∞), and hence, another explanation is required for the curvature of their $J(c)$ function. After a number of possible causes for the nonlinearity of the $J(c)$ function not related to a change in the properties of the pointed end were ruled out, we conclude that under physiological salt conditions the changes in the apparent rate constants at the pointed end of actin filaments may be due to a change in the nucleotide content of the terminal actin molecule from ADP to ATP. We successfully fit the data with a slightly simplified version of the model by Pantaloni et al. [Pantoloni, D., Carlier, M. F., & Korn, E. D. (1985) *J. Biol. Chem. 260*, 6572–6578].

In vivo the regulation of actin assembly and disassembly under physiological conditions depends on actin binding proteins (Stossel et al., 1985; Pollard & Cooper, 1986) and the kinetic properties of actin filaments (Korn, 1982; Mooseker, 1985). For instance, the fact that one actin filament end binds monomers more strongly than does the other (Wegner, 1976) has the result that capping of the preferred end by a binding protein produces partial filament disassembly (Kirschner, 1980; Coluccio & Tilney, 1983; Walsh et al., 1984b). This difference in monomer binding between the two ends (Pollard & Mooseker, 1981; Bonder et al., 1983; Doi & Frieden, 1984) is made possible by the ATPase activity of actin. Lately, attention has been focused on another consequence of the ATPase activity of actin filaments, which could be useful for regulation. Recent studies have indicated that the nucleotide content of the terminal F-actin molecules at the barbed end changes from ADP to ATP with increasing monomer concentrations (Pollard & Weeds, 1984; Carlier et al., 1984), leading to a concomitant change in the apparent rate constants of monomer binding and release (Carlier et al., 1984, 1985; Pollard, 1984; Walsh et al., 1984a). This was analyzed quantitatively by Carlier and her colleagues (Carlier et al., 1984, 1985), who found that the rate of elongation at the barbed filament end was not a linear function of the monomer concentration. Instead, the slope increased sharply below c_∞, indicating that the rate of depolymerization at the barbed end increases about 10-fold when the terminal nucleotide is changed from ATP to ADP (Lal et al., 1984; Pollard, 1984; Carlier et al., 1984; Walsh et al., 1984a). The slope was changed at very high monomer concentrations when the rate of elongation became much faster than the hydrolysis rate so that stretches of F-ATP-actin molecules were assembled (Pardee & Spudich, 1982). They concluded that the apparent rate constants at the barbed end of the actin filament changed with increasing monomer concentrations, as the result of a change in the nucleotide of the terminal F-actin molecules from ADP first to two ATP-containing actin molecules and eventually to longer stretches of F-ATP-actin molecules (Pantaloni et al., 1985b). This is of interest because regulatory mechanisms may exist that take advantage of this behavior. For the same reason it would be desirable to know whether the terminal nucleotide at the pointed end also changes from ADP to ATP and how such a change affects the rate constants.

† This work was supported by NIH Grants HLB 15585 (Pennsylvania Muscle Institute) (J.N. and A.W.) and AM 25387 (M.S.M.) and March of Dimes Basic Research Grant 1-924 (M.S.M.).

* Author to whom correspondence should be addressed.

‡ University of Pennsylvania.

§ Drexel University.

∥ Present address: Department of Physics, Virginia Commonwealth University, Richmond, VA 23284.

⊥ Yale University.

0006-2960/87/0426-2537$01.50/0

We present here a study of the kinetics of monomer uptake and release at the pointed end under physiological conditions (i.e., in the presence of 2 mM Mg^{2+} and 0.1 M K^+), using actin filaments capped at the barbed end by villin, a capping protein found in the intestinal microvilli [cf. Mooseker (1985)]. Our data suggest that at the pointed end the bound nucleotide of the terminal actin molecule may also change from ADP to ATP at higher monomer concentrations although ADP appears to be the terminal nucleotide at steady-state monomer concentrations. We further show that nuclei prepared from actin polymerized with villin at an actin–villin ratio of three (VA_3) started to elongate at lower monomer concentrations than did longer villin-capped actin filaments containing 18 or more actin molecules per villin, VA_{18}. This is because, in the presence of a nucleating substance like villin, filament assembly occurs by "linear" polymerization described by Oosawa [cf. Oosawa and Asakura (1975))]; i.e., at each monomer concentration a steady state is established between monomeric actin and villin–actin oligomers and polymers (Weber et al., 1987).

Experimental Procedures

Actin Preparations. Actin was prepared, chromatographed, stored, and modified with *N*-ethylmaleimide, NBD-Cl,[1] or pyrenyliodoacetamide as previously described (Northrop et al., 1986). Chromatographed actin used for experiments was kept for 2–4 weeks at 4 °C in column buffer containing 5 mM triethanolamine, pH 7.5, 0.5 mM ATP, 0.2 mM $CaCl_2$, 0.1 mM CaEDTA, and 6 mM NaN_3 (G buffer).

Villin was prepared according to Coleman and Mooseker (1985) and stored for several weeks at 4 °C. Fresh dithiothreitol was added to a concentration of 0.1 mM once a week. The activity of villin was followed by titrating 3 μM actin with villin to obtain the maximal increase in the steady-state monomer concentration, i.e., to find the villin–actin ratio with the lowest fluorescence increment. With fresh villin this was usually about 1/800. Villin was rejected when this ratio had fallen to 1/600.

Protein concentrations for villin and actin were calculated from E_{280} = 123.5 mM^{-1} cm^{-1} for villin and E_{290} = 24.9 mM^{-1} for actin. The concentration of pyrenylactin was corrected for the absorption of the probe according to Selden and colleagues (Shelden et al., 1983).

Fluorescence and Kinetic Measurements. Fluorescence measurements were carried out as previously described (Walsh et al., 1984a): excitation–emission wavelengths were 360–410 nm for pyrenylactin and 470–530 nm for NBD-actin. Light scattering artifacts were minimized by 390- and 490-nm cut-off filters in the emission path for pyrenylactin and NBD-actin, respectively. Experiments were carried out at 14 °C in polymerizing buffer containing 0.5 mM ATP, 10 mM Tris-HCl, pH 7.4 or 7.6, 2.0 mM $MgCl_2$, 0.1 M KCl, and $CaCl_2$ as indicated for each experiment. Prior to polymerization, G-actin was converted to Mg-actin; i.e., the tightly bound calcium was exchanged for magnesium as previously described (Northrop et al., 1986). In brief, G-actin was preincubated for 15–25 min in a medium containing EGTA equivalent to calcium and 500 μM magnesium at low G-actin and 100 μM magnesium at high G-actin concentrations. The conversion to Mg-actin was indicated by a small fluorescence *decrease* of the pyrenylactin to a new steady level. The lowering of magnesium at high G-actin concentrations was necessary in order to avoid a gradual fluorescence increase with time, indicating gradual polymerization of the actin.

Villin-capped actin oligomers and polymers were prepared by polymerizing 10 μM Mg-actin with villin at the desired actin–villin ratio, calculated on the basis of protein concentration, 18–24 h prior to use, in the presence of 0.1 M KCl, 2.0 mM $MgCl_2$, and 200 μM calcium. ATP levels were maintained by 5.0 mM creatine phosphate and 0.1 mg/mL creatine phosphokinase. For the determination of the critical concentration (c_∞), increasing concentrations of actin were allowed to polymerize at 16–19 °C for a period of 18 h. In the presence of villin the value for the critical concentration was obtained by extrapolation of the linear part of the curve (Weber et al., 1987).

Calculations. The G-actin concentration during the time course of elongation was calculated according to the expression $[G_0] - \Delta\text{emission}/b$, where $[G_0]$ is the starting G-actin concentration, which includes G-actin introduced with the filaments, Δemission is the fluorescence change, and b is the molar fluorescence of F-ADP-actin. The latter was obtained from the slope of a plot of fluorescence vs. total actin of the actin mixture used for the experiment. (This slope gives the fluorescence of F-ADP-actin since actin filaments have been shown to consist essentially of F-ADP-actin. The existence at steady state of at least one terminal F-ATP-actin molecule, possibly two, contaminates the fluorescence value by maximally 4% at average filament lengths of 50 monomers or more per filament.) This calculation gives accurate values for the G-actin concentration when each G-actin molecule was taken up by a filament end and none was used to form a villin–actin dimer from monomers and free villin present in the nucleating mixture. G-Actin uptake due to VA_2 formation would be underestimated since the pyrenyl fluorescence of two actin molecules in each villin–actin oligomer is very low (Weber et al., 1987). If, however, the two low-intensity molecules are in place already, then the uptake of every additional monomer gives a net increase in the total number of F-ADP-actin molecules and a net increase in the total fluorescence equal to that of one F-ADP molecule. This is so even if the monomer retains its bound ATP after binding and therefore increases its fluorescence intensity by only half as much as an F-ADP-actin molecule because at the same time the former terminal molecule also doubles its fluorescence after hydrolysis of its bound ATP.

Derivation of the Elongation Equations. The rate of elongation of filaments as a function of monomer concentration, $J(c)$, is defined as the rate of uptake of monomers from solution, divided by the number concentration of filaments, c_T:

$$J(c) = -(dc/dt)/c_T \quad (1a)$$

where c is the concentration of G-actin. In the simplest model [cf. Oosawa and Asakura (1975)], containing a single filament species

$$J(c) = k_+c - k_- \quad (1b)$$

In this model, hydrolysis is either so fast or so slow that all terminal actin molecules contain either ADP or ATP. In a model introduced by Pantaloni et al. (1985b), the rate constant for ATP hydrolysis k_H is of a similar magnitude as the rate constant of elongation at the barbed end. It was assumed that the two terminal actin molecules contain ATP as bound nucleotide, which hydrolyzes only very slowly. Rapid hydrolysis was postulated to occur only when a third F-ATP molecule is added at the end. The site of rapid hydrolysis is restricted

[1] Abbreviations: EGTA, ethylene glycol bis(β-aminoethyl ether)-*N*,*N*,*N*′,*N*′-tetraacetic acid; NBD-Cl, 7-chloro-4-nitro-2,1,3-benzoxadiazole; NEM, *N*-ethylmaleimide; EDTA, ethylenediaminetetraacetic acid; Tris-HCl, tris(hydroxymethyl)aminomethane hydrochloride.

to the molecule at the interface with the last internal F-ADP-actin molecule. This gives rise to a stable F-ATP-actin cap, as long as the rate of ATP hydrolysis at the interface is faster than the net rate of elongation of filaments.

To fit the simpler shape of the elongation curve observed for the pointed end, we employed a simplified model with a terminal F-ATP-actin cap of one rather than two. That is, hydrolysis is still assumed to occur only at the interface between the ADP body and the ATP cap of the filament but at one step earlier than in the model of Pantaloni et al., namely, when only two ATP-actin molecules are attached, i.e., for F_2. Then, to conform to the model, all the rate constants for F_2 and beyond are taken to be the same. For comparison with that model, we assume that the rate constants for the species in which hydrolysis occurs, which we assume to be F_2, will be the same as the species in their model for which hydrolysis occurs, namely, F_3. This means that k_2 is the rate of ATP-actin monomer addition to the end of species F_0 and k_{-2} is the rate of monomer release from species F_1. k_3 is the rate of ATP-actin monomer addition to the end of species with one or more ATP-actin molecules on the end, i.e., F_1 or larger, and k_{-3} is the rate of monomer release from species F_2 or larger. The constants k_1 and k_{-1} are not used in this simpler model. The steady-state rate of elongation with these assumptions is given by

$$J(c) = \frac{-k_{-0}(1 - K'c) + k_H K_2 K' c^2}{1 + (K_2 - K')c} \quad (2)$$

where k_{-0} is the rate constant for monomer release from species F_0, which has an ADP end, k_H is the rate of ATP hydrolysis at the interface between the cap and the ADP internal filament, as described above, and $K_2 = k_2/k_{-2}$. As in the more complex model, $K' = 1/c' = k_3/(k_H + k_{-3})$. Above c' the hydrolysis rate is small compared to the net rate of elongation and

$$J(c) = k_H + k_3(c - c') \quad (3)$$

In our fitting of the data, only eq 2 was used, since the values for c used were smaller than those for c'.

Results

We determined the monomer concentration dependence of the elongation rate for the pointed filament end using villin-capped actin filaments (Figure 1). Filaments of an average length of 18 actin molecules per villin (VA_{18}), when added to G-actin, elongated at their maximal rate without a lag period. This initial rate could not be recorded directly because the process of mixing extended into the initial phase of the reaction. However, it was ascertained by linear extrapolation of the first segment of the recorded fluorescence trace to zero time (data not shown). The line extrapolated to the initial fluorescence value, i.e., the value for the sum of the measured G-actin fluorescence corrected for dilution and the fluorescence of the added filaments. The extrapolation would have fallen below this value if there had been a lag period. The initial rate of elongation remained constant for a short period of time and did not decrease, although the monomer concentration began to decline as a result of monomer uptake. In Figure 1 we plotted the initial rate first against the added G-actin concentration and second against the average value of the corresponding G-actin concentrations.

Although the two plots are somewhat different from each other, they both are nonlinear and intersect the abscissa at the same value. This value was identical with the critical concentration, c_∞, obtained from the linear part of a graph of

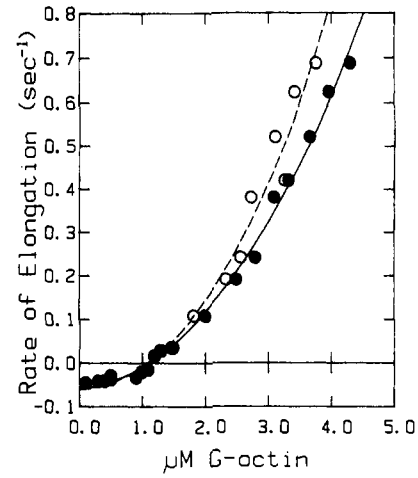

FIGURE 1: $J(c)$ function derived from initial rates of monomer uptake and release with increasing monomer concentrations. (Closed circles) Rates vs. added G-actin; (open circles) rates vs. average G-actin concentration assocd. with the initial rate. Temperature-equilibrated villin-capped actin filaments of an average size of 18 actin molecules per villin were diluted to a final concentration of 40 nM actin filament (=[villin]) into magnesium G-actin of increasing concentrations, with the simultaneous addition of salts to give final concentrations of 0.2 mM $CaCl_2$, 2.0 mM $MgCl_2$, and 0.1 M KCl. The rate of the fluorescence change of pyrenylactin (pyrenylactin:NEM-actin = 1:9) was measured at 14 °C. The data were converted to monomer uptake per villin per second. The curves connecting the data points were calculated with the equations developed by Pantaloni and his colleagues (Pantaloni et al., 1985b) to describe elongation at the barbed end and by adapting the parameters to fit the data. The following constants were used (for definition, see Experimental Procedures): (solid curve) $k_{-0} = 0.059\ s^{-1}$, $K' = 0.23\ \mu M^{-1}$, $K_2 = 0.21\ \mu M^{-1}$, and $k_H = 0.74\ s^{-1}$; (dashed curve) $k_{-0} = 0.06\ s^{-1}$, $K' = 0.21\ \mu M^{-1}$, $K_2 = 0.16\ \mu M^{-1}$, and $k_H = 1.2\ s^{-1}$.

fluorescence vs. total actin (Weber et al., 1987). This indicates that VA_{18} did not contain free villin or villin–actin monomers (see below). For the $J(c)$ curve of Figure 1, this would be the off-rate constant for F-ADP-actin molecules from the pointed end over the on-rate constants of ATP–actin monomers to pointed ends terminated by F-ADP-actin $[(k_{-0} + k_{-1})/k_1]$. The prominent feature of the $J(c)$ plot is the sharp decline in slope at G-actin concentrations below c_∞. In contrast, the $J(c)$ plot for the barbed end shows a sharp increase in slope below c_∞ (Carlier et al., 1984).

In view of the observation that the initial rate of elongation was maintained over a greater range of monomer concentrations than expected, we measured elongation rates during the whole time course of elongation as a function of the declining monomer concentrations during monomer uptake. The different symbols in Figure 2 show the data from several measurements of the time course of elongation, each starting at a different initial G-actin concentration. These $J(c)$ plots show only a positive phase because during the time course of depolymerization the number concentration of filaments decreased, whereas the interpretation of the $J(c)$ plot in terms of apparent rate constants requires a constant filament concentration. The data in Figure 2 are scattered around the curve that describes the initial rate of monomer uptake as a function of the corresponding average monomer concentration.

In a narrow region of monomer concentrations on either side of c_∞, the rate changed direction during the course of the reaction (Figure 3). An initial phase of fluorescence decrease of the filaments was followed by a short period of fluorescence increase. The net result of both phases was either a small net decrease of fluorescence at the lower G-actin concentrations or a small increase at the higher G-actin levels. The change in the direction of the reaction could not have been associated

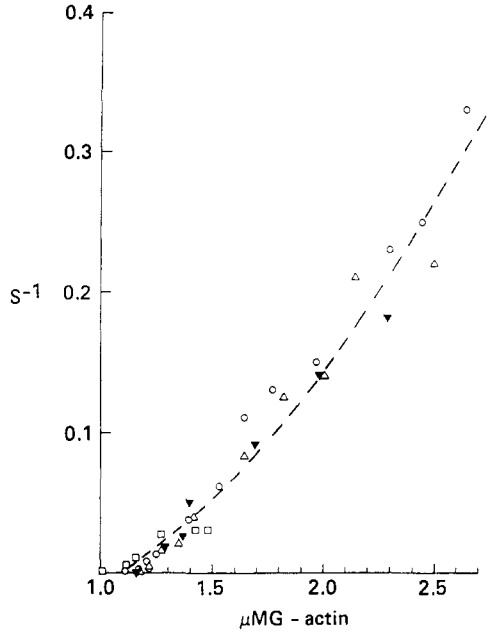

FIGURE 2: $J(c)$ function derived from the rates of monomer uptake as a function of declining monomer concentration during the time course of an elongation measurement. The starting G-actin concentrations were 3.1 (○), 2.8 (△), 2.5 (▽), and 1.5 μM (□). In several instances during the experiment of Figure 1 the whole time course of elongation was followed. Rates were measured at various times and plotted against the corresponding average G-actin concentration. The dashed line is taken from Figure 1. It is the curve relating the initial rates to the corresponding average, rather than the added, G-actin concentration. The monomer concentrations at the end point of elongation were 1.1 (○), 1.17 (△), 1.16 (▽), and 1.0 μM (□). The average value for all the end points in the experiment of Figure 1 was 1.1 μM.

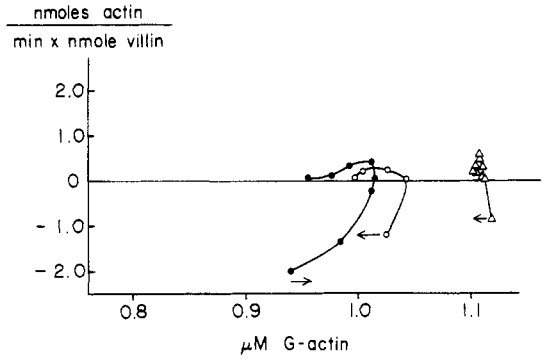

FIGURE 3: Rate reversal at added monomer concentrations near c_∞. The time course of monomer uptake and release at different G-actin levels was followed as described for Figures 1 and 2. Arrows indicate the direction of the overall change in monomer concentration, i.e., net depolymerization when pointing to higher and net elongation when pointing to lower monomer concentrations. Maximal possible reduction in average filament size at the transition from negative to positive rate from 18 to 16 (●), 18 to 17.5 (○), and 18 to 17.8 (△).

with a significant decrease in filament size. Translating the extent of the initial fluorescence decrease into the number of monomers released shows that the greatest change was a reduction in average size from 18 to 16 actin molecules per villin, whereas the smaller extent of depolymerization amounted to less than one monomer per villin.

Pursuing the question why, as mentioned above, initially the rate of fluorescence increase did not decline with decreasing G-actin concentrations, we investigated the possibility that, during the initial phase of elongation, stretches of F-ATP-actin may have been formed, as described by Carlier and her colleagues (Carlier et al., 1985), for barbed filament ends at very high G-actin concentrations. Then the initial rate of monomer uptake would have been underestimated because F-ATP-actin has a 50% lower pyrenyl fluorescence than F-ADP-actin (Carlier et al., 1984). The later rate would have been overestimated because the increase in pyrenyl fluorescence, during the gradual hydrolysis of F-ATP-actin to F-ADP-actin, would have been incorrectly attributed to monomer uptake at the time of ATP hydrolysis. Taking advantage of the fact that the fluorescence of NBD-F-actin does not distinguish between F-ADP-actin and F-ATP-actin (Carlier et al., 1984), we compared, in parallel experiments, the fluorescence change of pyrenylactin and NBD-actin during elongation measurements at relatively high G-actin concentrations (Table I). Using actin mixtures with both NBD-actin and pyrenylactin, we converted the fluorescence data from each probe to elongation rates on the basis of the molar fluorescence for F-ADP-actin. If all of the polymerized actin had retained its ATP, the elongation rates calculated from pyrenyl fluorescence changes would have been half of those calculated from NBD fluorescence increments. We observed no difference between the two probes at 4.4 μM G-actin. At 5.7 μM, the elongation rate calculated for pyrenylactin was 6% lower than that for NBD-actin. This translates into 12% F-ATP-actin, i.e., on the average 2.5 F-ATP-actin molecules per filament end (Table I). However, in view of the small size of the changes in NBD fluorescence (Table I), this number should be taken as nothing more than an indication that the fraction of F-ATP-actin present during elongation was not large.

Table I: Test for Accumulation of ATP-Actin Molecules at the Pointed Filament End

[G-actin] (μM)	time period (s)[a]	fluorescence units[b]		monomers[c]/villin in 20 s	
		pyrene	NBD	pyrene	NBD
4.4	20–40	18	5	15	15
5.7	20–40	23	7	19.7	21

[a] Period after initiation of elongation during which the rates were compared. [b] Duplicate measurements which gave the same values. [c] The rates in monomers per villin in 20 s were calculated from the fluorescence change with the molar emission for F-ADP-actin. Conditions: 36 nM villin; actin–villin ratio of nuclei for polymerization of 5; pyrenylactin:NBD-actin:NEM-actin = 1:2:7.

Table II: Elongation Rates as a Function of Monomer Concentration ($[G_0]$)

villin–actin nuclei	$[G_0]$ (μM)	n mol of actin bound/ villin × min
V[a]	1.8	0.4
VA_3	1.8	4.6
VA_{20}	1.8	4.6
V	2.3	1.2
VA_3	2.3	8
VA_{20}	2.3	9.5
V	2.7	1.4
VA_3	2.7	11
VA_{20}	2.7	13.4

[a] Villin only; aliquots of villin or villin–actin mixtures with an F-actin–villin ratio of 3 or 18 were diluted to a final concentration of 9 nM villin into G-actin. Pyrenylactin:NEM-actin = 1:1.

Reduction of the average length of the villin-capped filaments used as nuclei for elongation measurements, to below 10 molecules per villin, resulted in a different $J(c)$ plot (Figure 4). At an average oligomer length of three F-actin molecules per villin, VA_3, elongation started at a lower G-actin concentration than did the elongation of VA_{18}, and the monomer concentration at the abscissa intercept was lower than the independently determined value for c_∞. This indicates the presence of actin-binding species that are at steady state with monomer concentrations lower than c_∞ for pointed filament

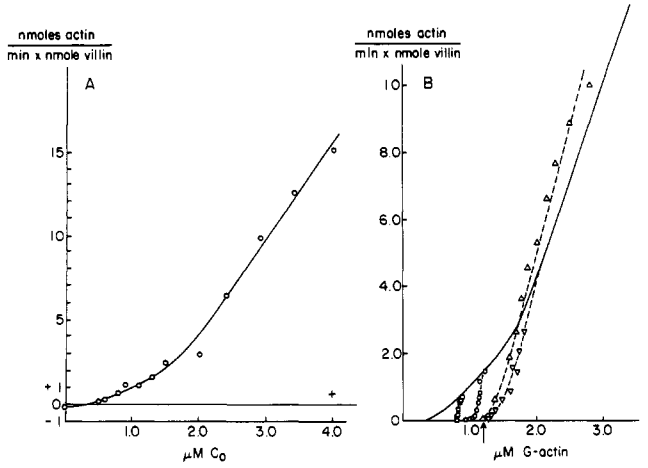

FIGURE 4: $J(c)$ plot with VA_3 as nuclei for elongation. The measurements in (A) and (B) were carried out as described for Figures 1 and 2, respectively, with VA_3 instead of VA_{18}. (A) The rates were measured when mixing was complete 10–20 s after addition of the oligomers to G-actin. The rates were plotted against the corresponding G-actin concentrations. (+) Rate in the absence of villin at 4.0 μM G-actin, initiated by spontaneous nucleation. (B) $J(c)$ function during the time course of elongation. The solid line without symbols is the curve in (A). The arrow denotes c_∞, obtained from the linear part of the plot showing the fluorescence at the end point after 18 h incubation as a function of total actin (data not shown). Conditions: 49 nM villin; pyrenylactin:NBD-actin = 1:1. The rates were calculated from the pyrenyl fluorescence. The final ratios of F-actin over total villin, [F]/[V], increased with increasing starting concentration of G-actin, $[G_0]$. Data denoted by (□) had $[G_0]$ = 0.8 μM and final F/V = 4.9; data denoted by (○) had $[G_0]$ = 1.29 μM and final F/V = 9.6; data denoted by (▽) had $[G_0]$ = 1.95 μM and final F/V = 20.0; data denoted by (△) had $[G_0]$ = 2.9 μM and final F/V = 34.0.

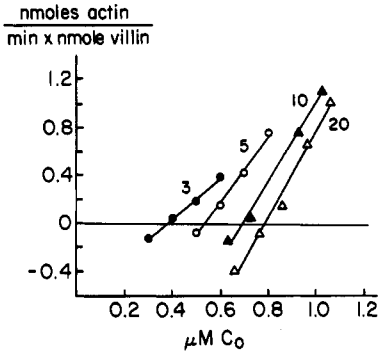

FIGURE 5: Effect of increasing the average size of the villin–actin polymers on the abscissa intercept of $J(c)$ plots. c_0 = added G-actin concentration. Numbers indicate the ratio of total actin over total villin. The experiments were carried out as described in Figure 1. The rates were calculated from pyrenyl fluorescence changes; however, calculations on the basis of NBD fluorescence gave the same abscissa intercepts. Conditions: 30 nM villin; pyrenylactin:NBD-actin = 1:1.

ends. The monomer concentration at the abscissa intercept increased with increasing actin–villin ratio until, at a ratio of 18, it equaled the value for c_∞ (Figure 5). The initial rates of elongation of VA_3 remained faster than those of VA_{18} until the two rates crossed over at G-actin concentrations which varied in different experiments between 1.5 and 1.8 μM (Table II; Figure 4B). At higher G-actin concentrations, the initial elongation rate of VA_3 was slower than that of VA_{18}. The latter suggests that the number of pointed ends was smaller for VA_3 than for VA_{18}. This is consistent with the observation that, at an actin–villin ratio of 3, a significant fraction of the total villin remains free (Weber et al., 1987). The reason is that, as will be shown below, free villin is not a nucleus; i.e., free villin binds actin more slowly than do the pointed ends (see below).

The $J(c)$ plot for VA_3 changed considerably when the elongation rates were followed during the time course of elongation as a function of the declining monomer concentration (Figure 4B). When the initial G-actin concentrations were below c_∞, elongation rates fell off rapidly with time, although the decline in monomer concentration due to monomer uptake was very small. Starting with G-actin concentrations greater than 2.0 μM, the rates initially increased for a brief period in spite of decreasing monomer levels (data not shown). This probably reflects the conversion of free villin to VA_2, which binds monomers more rapidly than does villin (see below) and with a greater fluorescence increment than that associated with the formation of VA_2. During continued elongation, the $J(c)$ plot for VA_3 became the same as that for VA_{18}, and the rate of elongation became zero at c_∞ for the pointed end rather than at the lower G-actin concentration as observed during measurements of initial rates.

To check that free villin was not a nucleus, we compared initial rates of monomer uptake by free villin with those by VA_3 and by VA_{18}. The data in Table II show that free villin bound actin much more slowly than did VA_3 or VA_{18}. These rates speeded up with time, as has been observed for other capping proteins (Cooper & Pollard, 1985). The initial rates of actin binding by free villin in Table II, however, cannot be used to calculate the rate constant of association because of two complicating factors. First, in this particular actin preparation, some spontaneous nucleation contributed to the fluorescence change. This could not be accurately corrected for by control experiments in the absence of villin. In the presence of free villin, the elongation rate of spontaneously formed nuclei would be smaller than in the control because the barbed ends of these nuclei would presumably be capped by the free villin. Monomer uptake by spontaneously formed nuclei makes the rate of actin binding by free villin appear to be higher than it really was. The second complicating factor is the very low, 4-fold rather than 30-fold (Weber et al., 1987) increase in fluorescence intensity associated with the binding of the first two pyrenylactin molecules to villin, which leads to an underestimation of the initial rate of actin binding to villin. An accurate correction for this factor was not possible since it was not known how much VA_2 had been formed at any time as compared with larger villin–actin oligomers. However, the rate of monomer binding to villin was estimated to be only $^1/_3$ of that by VA_{18}, even when an overcorrection for the binding of the first two actin molecules to villin had been made, by assuming that the appearance of F-ADP-actin fluorescence was preceded by complete saturation of villin with two actin molecules.

Discussion

The main observation in this study is that, under physiological salt conditions, the elongation rate of villin-capped actin filaments does not increase linearly with increasing monomer concentration. A plot of the elongation rate vs. monomer concentration, the $J(c)$ plot [cf. review of Hill and Kirschner (1982)], is linear when there is no change in the properties of the polymer, so that the elongation rate increases in linear proportion to the increase in monomer concentration. Our observation of a nonlinear $J(c)$ plot at first appears to be comparable with the findings in several studies from Korn's laboratory (Coué & Korn, 1985, 1986; Carlier et al., 1986) that appeared while this paper was in preparation. These studies show, in the absence of potassium, nonlinear $J(c)$ functions for filaments blocked at their barbed ends by two different barbed-end cappers. However, the mechanism underlying the nonlinearity of the $J(c)$ function appears to be

different under physiological conditions, as in our experiments, and in the absence of potassium, as in the experiments from Korn's laboratory. Our data suggest that the nonlinearity is due to a change in the properties of the pointed filament end with increasing monomer concentrations, presumably a change in the bound nucleotide of the terminal actin molecule from ADP to ATP. By contrast, Korn and his colleagues show that, in the absence of potassium, the curvature is due to reasons unrelated to the properties of the pointed filament end and that therefore the bound nucleotide is ADP at all monomer concentrations between 0 and 20 μM (Coué & Korn, 1985).

In the following we shall discuss various causes for the nonlinearity of a $J(c)$ plot that are not related to the properties of the pointed ends. The first possible cause may be a contamination of the pointed ends with barbed ends at increasing monomer concentrations. Displacement of some of the caps by increasing G-actin concentrations is given as the explanation for the curvature of the $J(c)$ plot when actin filaments are capped by cytochalasin D (Carlier et al., 1986). In our case, barbed filament ends could only be generated by spontaneous nucleation since villin, with a binding constant to filament ends of 10^{11} M^{-1} (Walsh et al., 1984a) and a rather low monomer binding constant (Weber et al., 1987), remains bound to filament ends at all monomer concentrations. Spontaneous nucleation cannot be accurately corrected for by subtracting elongation rates measured in the absence of capper. The reason is that spontaneous nuclei formed in the absence of capper elongate rapidly at their barbed ends, whereas, in the presence of a capping agent, some spontaneous nuclei would probably be capped by binding of the agent to the barbed filament ends. Therefore, we tried to avoid spontaneous nucleation by using actin preparations that had lag periods of 90 s in the absence of villin at the highest monomer concentration used. Further evidence that spontaneous nucleation did not affect the results are the $J(c)$ plots taken during the time course of elongation. An elongation rate measured at some time during filament elongation when the G-actin concentration has decreased to some new value G' will only equal the initial elongation rate for concentration G' if there has been insignificant spontaneous nucleation of filaments. In this context it should be remembered that spontaneous nucleation increases as a power of the monomer concentration [cf. Oosawa and Asakura (1976), Cooper et al. (1983), Frieden (1983), and Tobacman and Korn (1983)].

Second, we considered an increase in the number concentration of villin–actin nuclei with increasing actin concentrations as a possible cause for the nonlinearity of the $J(c)$ function. This is how Coue and Korn (1985, 1986) explain the curvature for gelsolin-capped actin filaments in the absence of potassium. This is the cause for much of the exaggerated curvature observed when VA_3 was used to nucleate elongation (Figure 4). An increase in the concentration of villin–actin nuclei with increasing G-actin concentrations, however, as will be discussed below, does not explain the nonlinearity with VA_{18} as nuclei. If the average size is VA_3, then the solution consists of a mixture of free villin, VA_2, and villin–actin oligomers of larger sizes in equilibrium with monomeric actin (Weber et al., 1987). With increasing monomer concentrations, the equilibrium shifts toward VA_2 and VA_n, which are nuclei for elongation, and away from free villin, which is not a nucleus since it was shown to have a lower on-rate constant for monomer binding than that of the pointed filament ends (Table II). The adjustment of the equilibria took place, in part, during the initial rate measurements, which took a finite period of time. VA_3 elongated below c_∞, first, because free villin increasingly bound monomers to form VA_2 and, second, because VA_2 and larger oligomers elongated to an extent appropriate to the increase in the product K_∞ [G-actin] (Weber et al., 1987). Elongation at G-actin concentrations below c_∞ is a sensitive indicator for the presence of a significant concentration of prenuclei such as free villin or villin–actin monomers (Weber et al., 1987). The total amount of monomer uptake required to adjust the equilibrium at G-actin concentrations below c_∞ was very small, and therefore, elongation at subcritical actin concentrations lasted only for a very short period. By contrast, at G-actin concentrations above c_∞ elongation continued until enough actin had been taken up to bring the G-actin concentration back to c_∞. At higher initial G-actin concentrations, all villin was converted to villin–actin nuclei. Therefore, the $J(c)$ function for VA_3 measured during the course of elongation eventually became comparable to that for VA_{18}.

The nonlinearity of the $J(c)$ plot with VA_{18} as nuclei for elongation cannot be explained in this manner, since it has been shown that the concentrations of free villin or VA are insignificant at these actin–villin ratios, whereas VA_2 is already a nucleus (Weber et al., 1987). This is supported, using the same reasoning applied to spontaneous nucleation, by the observation that the $J(c)$ plot was the same for initial rates and for the rates during the course of elongation when the G-actin concentrations changed as a result of monomer uptake by filament ends.

A third cause of nonlinearity unrelated to the properties of the pointed end was suggested by one of the reviewers. On the basis of the studies by Newman et al. (1985) and Mozo-Villaries (1985) showing the existence of very small amounts of oligomers at subcritical actin concentrations in the absence of added nucleating substances, he proposed that the concentrations of actin dimers and trimers may become quite large with increasing monomer concentration. As a result, the rate of elongation may be determined to a significant degree by the binding of dimers and trimers to pointed ends. This might explain the curvature of the $J(c)$ plot, since then at higher G-actin concentrations two or three actin molecules would be taken up simultaneously. This does not appear to have happened in our experiments because we showed that spontaneous nucleation did not interfere with our measurements. These oligomers would not only bind to pointed filament ends but also grow rapidly at their free barbed ends; i.e., they would give rise to spontaneous nucleation. Furthermore, during the conversion of calcium to magnesium actin, the fluorescence of both pyrenylactin and NBD-actin remained the same with increasing G-actin concentrations. This is especially significant for NBD-actin, since the villin- and the gelsolin-bound NBD-actin dimers have 50% (Weber et al., 1987; Bryan & Kurth, 1983) or 100% (Coué & Korn, 1985, 1986) of the fluorescence of NBD-F-actin. Furthermore, Godette and Frieden (1986) have recently shown that the actin dimers that are very slowly formed in the presence of magnesium do not participate in elongation.

Fourth, we should like to comment on the rate reversal after dilution of villin–actin filaments into G-actin solutions near c_∞. We have no explanation for this reversal, and therefore we cannot relate it to the $J(c)$ function. The rate reversal suggests that the steady state before and after dilution of the nuclei for elongation was different with respect to some parameter other than the total monomer concentration. On the basis of the experiments by Pantaloni et al. (1984), we calculated that there may have been more G-ADP-actin in the filament stock solution than in the medium used for the

elongation measurements. Pantaloni et al. (1984) observed the accumulation of G-ADP-actin at high concentrations of actin filaments under conditions where the rate constant for ADP–ATP exchange, with an estimated value of 0.005 s^{-1}, was very low. In the presence of potassium and magnesium, the exchange rate constant must have been at least 20 times higher to be compatible with our measurements. These are measurements of NBD fluorescence showing no increase in the critical concentration of villin-capped actin filaments when the filament concentration was raised from 10 to 1000 nM (Weber et al., 1987; Figure 4). Nevertheless, with a value of 0.1 s^{-1} for the exchange rate, the concentration of G-ADP-actin was calculated to have been 0.25 μM in the filament stock solution as compared to 0.01 μM in the assay medium (1.1 μM total G-actin in both solutions). However, we know of no data that would allow us to speculate how a sudden fall in the concentration of G-ADP-actin results in a transient decrease of fluorescence followed by an increase.

In view of the outcome of all these control experiments, we feel justified in attributing the observed nonlinearity of the $J(c)$ plot under physiological salt conditions to a change in the bound nucleotide of the terminal actin molecule from ADP to ATP with increasing monomer concentrations. In an elegant study, Coué and Korn (1986) recently showed, by direct comparison of the rates of ATP hydrolysis and elongation, that, in the absence of potassium, gelsolin-capped actin filaments acquire stretches of F-ATP-actin molecules at monomer concentrations above 10 μM. Our experiments suggest that this G-actin concentration is significantly lower in the presence of potassium.[2] We fit the data collected for the $J(c)$ function with the expressions developed by Pantaloni and his colleagues for the barbed filament end (Pantaloni et al., 1985b) (cf. Experimental Procedure) (Figure 1). The purpose of fitting the data with eq 2 was to demonstrate that the data could, in fact, be rationalized by a mechanism based on the hydrolysis–cap model of Pantaloni and his colleagues (Pantaloni et al., 1985b). It is clear that the shape of the curve does not strictly require four parameters. This means that the parameters chosen in the fitting process will not be unique and, moreover, changes in some of the parameters can be compensated by correlated changes in the others. It is of interest, however, that reasonable parameters provide an excellent fit. Further work is necessary to determine whether a simpler model can be constructed that fits the data equally well with fewer parameters. In this context, it should also be noted that the simplified model employed here can fit the published data of Pantaloni et al. (1985b) with accuracy almost equivalent to that of the model that they employed, which had one additional parameter.

ACKNOWLEDGMENTS

We thank Frank Tilli for the preparation and quality control of the actin preparations. We are indebted to Joseph Bryan for his critical reading of the manuscript and for stimulating discussions.

REFERENCES

Bergen, L. G., & Borisy, G. G. (1980) *J. Cell Biol. 84*, 141–150.

Bonder, E. M., Fishkind, D. J., & Mooseker, M. S. (1983) *Cell (Cambridge, Mass.) 34*, 491–501.

Carlier, M. F., Pantaloni, D., & Korn, E. D. (1984) *J. Biol. Chem. 259*, 9983–9986.

Carlier, M. F., Pantaloni, D., & Korn, E. D. (1985) *J. Biol. Chem. 260*, 6565–6571.

Carlier, M. F., Criquet, P., Pantaloni, D., & Korn, E. D. (1986) *J. Biol. Chem. 261*, 2041–2050.

Chaparala, S., Mooseker, M. S., Northrop, J., Walsh, T. P., & Weber, A. (1987) *Cell Motil.* (submitted for publication).

Coleman, T. R., & Mooseker, M. S. (1985) *J. Cell Biol. 101*, 1850–1857.

Coluccio, L. M., & Tilney, L. G. (1983) *J. Cell Biol. 97*, 1629–1634.

Cooper, J. A., & Pollard, T. D. (1985) *Biochemistry 24*, 793–799.

Cooper, J. A., Buhle, E. L., Walker, S. B., Tsong, T. X., & Pollard, T. D. (1983) *Biochemistry 22*, 2193–2202.

Coué, M., & Korn, E. D. (1985) *J. Biol. Chem. 260*, 15033–15041.

Coué, M., & Korn, E. D. (1986a) *J. Biol. Chem. 261*, 1588–1593.

Coué, M., & Korn, E. D. (1986b) *J. Biol. Chem. 261*, 3628–3631.

Doi, Y., & Frieden, C. (1984) *J. Biol. Chem. 259*, 11868–11875.

Frieden, C. (1983) *Proc. Natl. Acad. Sci. U.S.A. 80*, 6513–6517.

Godette, D. W., Uberbacher, E. C., Bunick, G. J., & Frieden, C. (1986) *J. Biol. Chem. 261*, 2605–2609.

Hill, T. L., & Kirschner, M. W. (1982) *Int. Rev. Cytol. 78*, 1–125.

Kirschner, M. W. (1980) *J. Cell Biol. 86*, 330–334.

Korn, E. D. (1982) *Physiol. Rev. 62*, 672–737.

Lal, A. A., Brenner, S. L., & Korn, E. D. (1984) *J. Biol. Chem. 259*, 13011–13015.

Mooseker, M. S. (1985) *Annu. Rev. Cell Biol. 1*, 261–293.

Mozo-Villaria, A., & Ware, B. R. (1985) *Biochemistry 24*, 1544–1548.

Newman, J., Estes, J. E., Selden, L. A., & Gershman, L. C. (1985) *Biochemistry 24*, 1538–1545.

Northrop, J., Weber, A., Mooseker, M. S., Armstrong, C., Bishop, M. F., Dubyak, G. R., Tucker, M., & Walsh, T. P. (1986) *J. Biol. Chem. 261*, 9274–9281.

Oosawa, F., & Asakura, S. (1975) *Thermodynamics of the Polymerization of Proteins*, Academic, New York.

Pantaloni, D., Carlier, M. F., Coué, M., Lal, A. A., & Brenner, S. L. (1984) *J. Biol. Chem. 259*, 6274–6283.

Pantaloni, D., Carlier, M. F., & Korn, E. D. (1985a) *J. Biol. Chem. 260*, 6572–6578.

Pantaloni, D., Hill, T. L., Carlier, M. F., & Korn, E. D. (1985b) *Proc. Natl. Acad. Sci. U.S.A. 82*, 7201–7211.

Pardee, J. D., & Spudich, J. A. (1982) *J. Cell Biol. 93*, 648–324.

Pollard, T. D. (1984) *J. Cell Biol. 99*, 769–777.

Pollard, T. D., & Mooseker, M. S. (1981) *J. Cell Biol. 88*, 654–659.

Pollard, T. D., & Weeds, A. G. (1984) *FEBS Lett. 170*, 94–98.

Pollard, T. D., & Cooper, J. A. (1986) *Annu. Rev. Biochem. 55*, 987–1035.

Selden, L. A., Estes, J. E., & Gershman, L. C. (1983) *Biochem. Biophys. Res. Commun. 116*, 478–485.

Stossel, T. P., Chaponnier, C., Ezzell, R. M., Hartwig, J. H., Janmey, P. A., Kwiatkowski, D. J., Lind, S. E., Smith, D.

[2] Whereas the omission of potassium appears to affect the kinetics at the barbed filament end only moderately, it significantly alters the rate constants at the pointed filament end, lowering k_+ 4–5-fold and increasing c_e for the pointed end by the same factor [cf. Coué and Korn (1985, 1986) with Walsh et al. (1984a) and with these data].

B., Southwick, F. S., Yin, H. L., & Zaner, K. S. (1985) *Annu. Rev. Cell Biol. 1*, 353–402.
Tobacman, L. S., & Korn, E. D. (1983) *J. Biol. Chem. 258*, 3207–3214.
Walsh, T. P., Weber, A., Higgins, J., Bonder, E. M., & Mooseker, M. S. (1984a) *Biochemistry 23*, 2613–2621.
Walsh, T. P., Weber, A., Davis, K., Bonder, E. M., & Mooseker, M. S. (1984b) *Biochemistry 23*, 6099–6102.
Weber, A., Northrop, J., Bishop, M. F., Ferrone, F. A., & Mooseker, M. S. (1987) *Biochemistry* (preceding paper in this issue).
Wegner, A. (1976) *J. Mol. Biol. 108*, 139–150.

Assignment of Fingerprint Vibrations in the Resonance Raman Spectra of Rhodopsin, Isorhodopsin, and Bathorhodopsin: Implications for Chromophore Structure and Environment†

Ilona Palings,‡ Johannes A. Pardoen,§ Ellen van den Berg,§ Chris Winkel,§ Johan Lugtenburg,§ and Richard A. Mathies*,‡

Chemistry Department, University of California, Berkeley, California 94720, and Chemistry Department, Gorlaeus Laboratories, Leiden University, 2300 RA Leiden, The Netherlands

Received August 22, 1986; Revised Manuscript Received December 12, 1986

ABSTRACT: ^{13}C- and ^{2}H-labeled retinal derivatives have been used to assign normal modes in the 1100–1300-cm^{-1} fingerprint region of the resonance Raman spectra of rhodopsin, isorhodopsin, and bathorhodopsin. On the basis of the ^{13}C shifts, C_8–C_9 stretching character is assigned at 1217 cm^{-1} in rhodopsin, at 1206 cm^{-1} in isorhodopsin, and at 1214 cm^{-1} in bathorhodopsin. C_{10}–C_{11} stretching character is localized at 1098 cm^{-1} in rhodopsin, at 1154 cm^{-1} in isorhodopsin, and at 1166 cm^{-1} in bathorhodopsin. C_{14}–C_{15} stretching character is found at 1190 cm^{-1} in rhodopsin, at 1206 cm^{-1} in isorhodopsin, and at 1210 cm^{-1} in bathorhodopsin. C_{12}–C_{13} stretching character is much more delocalized, but the characteristic coupling with the $C_{14}H$ rock allows us to assign the "C_{12}–C_{13} stretch" at ~1240 cm^{-1} in rhodopsin, isorhodopsin, and bathorhodopsin. The insensitivity of the C_{14}–C_{15} stretching mode to N-deuteriation in all three pigments demonstrates that each contains a trans (anti) protonated Schiff base bond. The relatively high frequency of the C_{10}–C_{11} mode of bathorhodopsin demonstrates that bathorhodopsin is s-trans about the C_{10}–C_{11} single bond. This provides strong evidence against the model of bathorhodopsin proposed by Liu and Asato [Liu, R., & Asato, A. (1985) *Proc. Natl. Acad. Sci. U.S.A. 82*, 259], which suggests a C_{10}–C_{11} s-cis structure. Comparison of the fingerprint modes of rhodopsin (1098, 1190, 1217, and 1239 cm^{-1}) with those of the 11-*cis*-retinal protonated Schiff base in methanol (1093, 1190, 1217, and 1237 cm^{-1}) shows that the frequencies of the C–C stretching modes are largely unperturbed by protein binding. In particular, the invariance of the C_{14}–C_{15} stretching mode at 1190 cm^{-1} does not support the presence of a negative protein charge near C_{13} in rhodopsin. In contrast, the frequencies of the C_8–C_9 and C_{14}–C_{15} stretches of bathorhodopsin and the C_{10}–C_{11} and C_{14}–C_{15} stretches of isorhodopsin are significantly altered by protein binding. The implications of these observations for the mechanism of wavelength regulation in visual pigments and energy storage in bathorhodopsin are discussed.

Rhodopsin, the major protein in the disc membranes of retinal rod cells, is the pigment responsible for black and white vision in vertebrates. The amino acid sequence of bovine rhodopsin has been determined (Hargrave et al., 1983; Ovchinnikov, 1982), and the secondary structure is thought to consist of seven transmembrane α-helices (Chabre, 1985). Rhodopsin contains an 11-*cis*-retinal chromophore bound to lysine-296 via a protonated Schiff base bond. Upon absorption of light the chromophore photoconverts to the all-trans isomer (I) forming the primary photoproduct bathorhodopsin, which

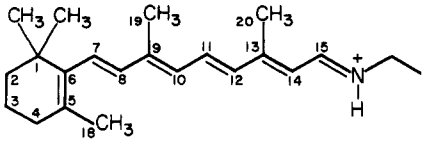

I

decays thermally via a series of metastable intermediates (Yoshizawa & Wald, 1963). The metarhodopsin II form catalyzes the activation of the enzyme transducin (Bennett et al., 1982), which carries the excitation signal to a phosphodiesterase (Stryer, 1986). The consequent reduction in the cytoplasmic cGMP level effects a closure of the sodium channels of the plasma membrane and results in the hyper-

† Work in Berkeley was supported by a grant from the National Institutes of Health (EY-02051). Work in Leiden was supported by grants from The Netherlands Organization for the Advancement of Pure Research (ZWO) and The Netherlands Foundation for Chemical Research (SON). R.A.M. is an NIH Research Career Development Awardee (EY-00219). Preliminary accounts of this work were presented at the 29th and 30th Annual Meetings of the Biophysical Society, February 1985 and 1986.

* Author to whom correspondence should be addressed.
‡ University of California.
§ Leiden University.

0006-2960/87/0426-2544$01.50/0